applied sciences

MDPI

Article

Simple Route to Increase Electrical Conductivity and Optical Transmittance in Graphene/Silver Nanoparticles Hybrid Suspensions

Egor A. Danilov [1], Mikhail Veretennikov [1], Maria Dronova [1,2,†], Timofey Kalyakin [1,3], Andrey A. Stepashkin [4], Victor V. Tcherdyntsev [4,*] and Vladimir Samoilov [1]

1 Research Institute for Graphite-Based Structural Materials "NIIgrafit" (JSC "NIIgrafit"), Elektrodnaya Street 2, Moscow 111524, Russia
2 Department of Special Machinery, Bauman Moscow State Technical University, 2nd Baumanskaya Str. 5, Moscow 105005, Russia
3 Faculty of Technology of Oil & Gas Chemistry and Polymer Materials, D. Mendeleev University of Chemical Technology of Russia, Miusskaya Sq. 9, Moscow 125047, Russia
4 Laboratory of Functional Polymer Materials, National University of Science and Technology "MISIS", Leninskii prosp, 4, Moscow 119049, Russia
* Correspondence: vvch@misis.ru; Tel.: +7-910-400-2369
† Current Affiliation: Skolkovo Institute of Science and Technology, Skolkovo Innovation Center, Bolshoy Boulevard 30, bld. 1, Moscow 121205, Russia.

Abstract: Electrical and optical properties of graphene/silver nanoparticles hybrid suspensions intended for use in inkjet printing technologies were studied. Few-layered graphene particles were manufactured via a direct ultrasonic-assisted liquid-phase exfoliation route in water/surfactant system, whereas silver nanoparticles were synthetized using a polyol process. Hybrid suspensions for graphene/silver nanoparticles mixtures showed significant reduction in mean particle size while electrical conductivity remained almost intact even after thorough centrifugation. Structuring effects in mixed colloids were very pronounced as both electrical conductivity and optical transmission showed maxima at 65 wt.% graphene. Suspensions with conductivities above 300 µSm/cm, much higher than previously reported, were obtained, and resulted in the manufacturing of films with less than 10% optical absorption throughout the visible region. These samples did not demonstrate absorption peaks attributed to silver nanoparticles' surface plasmon resonance, which is suitable for transparent electrode applications. Suspension properties at optimal composition (65 wt.% graphene) are very promising for printed electronics as well as transparent conductive coating applications. In the paper, we establish that the optimal suspension composition matches that of the film; therefore, more attention should be paid to carefully studying electrically conductive suspensions.

Keywords: graphene; silver nanoparticles; inkjet printing; transparent electrodes; electrical conductivity; optical absorption; centrifugation

check for updates

Citation: Danilov, E.A.; Veretennikov, M.; Dronova, M.; Kalyakin, T.; Stepashkin, A.A.; Tcherdyntsev, V.V.; Samoilov, V. Simple Route to Increase Electrical Conductivity and Optical Transmittance in Graphene/Silver Nanoparticles Hybrid Suspensions. *Appl. Sci.* **2023**, *13*, 1922. https://doi.org/10.3390/app13031922

Academic Editors: Babak Safaei, Zhaoye Qin, Tien-Chien Jen and Rasool Moradi-Dastjerdi

Received: 13 December 2022
Revised: 27 January 2023
Accepted: 29 January 2023
Published: 2 February 2023

Copyright: © 2023 by the authors. Licensee MDPI, Basel, Switzerland. This article is an open access article distributed under the terms and conditions of the Creative Commons Attribution (CC BY) license (https://creativecommons.org/licenses/by/4.0/).

1. Introduction

Electrically conductive suspensions are currently widely studied as a promising material for printed and flexible electronics, especially for inkjet printing technologies [1]. Although metal micro- or nanoparticles are generally used, graphene has been attracting a lot of attention as a promising material due to its excellent electrical and optical properties, chemical stability, and potential commercial availability [2]. Nevertheless, graphene, being a semimetal, shows a high level of local contact resistances that lead to increased sheet resistance of graphene-based films and limits their potential applications in both transparent conducting coatings and contact tracks for printed circuits [3]. Additionally, most of the studies are devoted to graphene oxide (GO) and reduced GO (RGO) [4,5] suspensions.

However, it is almost impossible to achieve a sufficiently high degree of reduction to minimize defects and oxygen-containing groups and provide high electrical conductivity of the particles. Direct liquid-phase exfoliation is a route that, at the cost of decreased yield of few-layered particles, does not lead to generation of defects in the graphene plane. Therefore, choosing highly crystalline graphite, such as natural graphite or highly oriented pyrolytic graphite (HOPG), enables one to obtain low-defect few-layered graphene particles directly in the form of stabilized suspensions. Numerous studies report N-methyl-2-pyrrolidone (NMP) [6,7] or dimethylformamide (DMF) [8] as preferable media for exfoliation. The choice of an eco-friendly exfoliation medium should, however, be also taken into account; therefore, water- or alcohol-based systems are much more preferable. Several studies report water-surfactant systems as being suitable for high-yield exfoliation [9,10]; the choice of surfactants is thoroughly treated in several studies as well [11,12].

On the other hand, silver nanoparticles (AgNPs) have extremely low electrical resistance and sintering temperatures. Moreover, being metals, AgNPs do not suffer from high local contact resistance. Their main drawbacks are deterioration in air and sulfur-containing gases, as well as a relatively high price. Several techniques have been described to achieve monodisperse spherical AgNPs, including cryosynthesis [13] and plasma-induced synthesis [14]. Many applications require AgNPs of different morphologies, which is challenging to achieve when the process is thermodynamically-controlled; therefore, chemical routes that provide kinetic control of particle growth should also be considered. Soft chemical methods, especially polyol synthesis, liquid-phase reduction of silver salts in polyhydroxyl alcohols, are more promising and widely used due to the opportunity to achieve fine control of the synthesis parameters so that spherical NPs [15], polyhedral AgNPs [16], or silver nanowires (AgNWs) [17] can be obtained at high selectivity and high yield.

High electrical conductivity values required for inkjet printing applications can be typically achieved only when dispersed particle concentrations are above the so-called percolation threshold [18]; on the other hand, at this level of concentration (12–30 vol.%) the viscosity of the system may limit applications as electrically conductive inks. Percolation theory suggests that mixed morphology systems with both rod- and spherical or platelet-shaped particles enable a significant reduction in percolation threshold concentration down to below 1–2 vol.%, so the system remains sufficiently diluted and has low viscosity. A certain amount of studies are devoted to the subject [19,20], and graphene/graphite-metal nanorods-based colloids seem to be the most promising. Most studies report that the higher the metal content is in a hybrid suspension, the higher the electrical conductivity; however, most studies operated in a limited concentration range. Nonetheless, several theoretical and experimental studies suggest that there should be an optimal component ratio in a 1D + 2D-morphology system [21–27].

Transparent conductive electrodes (TCE) widely used for photovoltaics [28], light-emitting diodes [29], sensor screens [30], smart windows [31], and antistatic coatings [32] seem to be particularly challenging as objects of flexible and printed electronics, as achieving both high electrical conductivity and high transparency is challenging even for ink formulations, let alone films. This happens because electrical conductivity increases with solid phase concentration; so, however, does optical absorption; thus, relatively low percolation thresholds are required from the suspension. Therefore, it is crucial to achieve an optimal conductive phase concentration that provides sufficient conductivity and transparency at the same time. Another important requirement for TCE applications is the maximization of optical spectrum smoothness, that is, the absence of absorption peaks in the visual region. Unfortunately, AgNPs are known for optical absorption peaks at 300–420 nm due to surface plasmon resonance (SPR) [33], which needs to be suppressed for effective use in TCE. There are several studies that addressed graphene-based nanoplatelets/metallic nanorods hybrid systems for manufacturing TCE for electromagnetic shielding [34], electromagnetic shielding [35], optoelectronic devices [36], light-emitting diodes [37], solar cell technologies [38–41], and display and various sensor devices [42–46]. Although much effort has been made to achieve combinations of high conductivity and high transparency in films, little data is published on the properties of the suspensions themselves, as well as on how the graphene/metal nanoparticle ratio affects the properties of suspensions and films derived from them.

In the present paper, we report hybrid few-layered graphene/AgNP electrically conductive suspensions in a mixed water-ethylene glycol (EG) system. Graphene suspensions were prepared via direct ultrasonic-assisted liquid-phase exfoliation in a water-surfactant system. AgNPs were manufactured via polyol synthesis in EG in the presence of polyvinylpyrrolidone (PVP) as a surface-stabilizing agent. It is shown that after mixing and ultrasonic treatment of the suspensions, AgNPs decorate the graphene surface. Particle size distributions, electrical conductivity, and optical absorption in the visible region were studied throughout the whole range of graphene:AgNP ratios (0–100 wt.%). In order to obtain the inks potentially suitable for TCE applications, we used mild centrifugation to separate large particles. Electrically conductive transparent suspensions showed a synergistic effect of both optical absorption and electrical conductivity. Films obtained from the suspensions were also characterized by optical and electrical resistance measurements.

2. Materials and Methods

Suspensions of few-layered graphene nanoparticles (FLG) were manufactured via a previously described [47] direct ultrasonic-assisted liquid-phase exfoliation route in deionized water with a fluorine-containing surfactant (Zonyl BA-L, Dupont, Wilmington, DE, USA). Natural graphite (GSM-2 brand) was used as a precursor. Graphite was heat-treated under vacuum at 2100 °C followed by high-temperature (2800 °C) treatment in a Freon R22 atmosphere in order to obtain >99.9 wt.% purity. Ultrasonication time was 6 h in all cases. A horn-type unit with acoustic power 200 W was used.

AgNPs were manufactured via polyol synthesis following the protocol described in [48]. Synthesis temperature was kept at 170 °C. Silver nitrate (extra pure 99.9+%, Lenreactiv, St. Petersburg, Russia), potassium bromide (99.9+%, Acros Organics, Geel, Belgium), ethylene glycol (EG) (extra pure, Acros Organics, Geel, Belgium) were used as precursors, whereas surface stabilizer polyvinylpyrrolidone (PVP) of low (M_w 8000, 99.995+% pure, Acros Organics, Geel, Belgium) molecular weightwas used. The PVP:$AgNO_3$ weight ratio was kept at 5:2. Synthesis was carried out in air.

In order to obtain transparent conductive suspensions, an EBA 280 centrifuge (Hettich, Beverly, MA, USA) was used, operating at cycles at 2000 rpm (whenever not specified, total centrifugation time was 30 min). Before centrifugation, each suspension was treated with ultrasound using a horn-type ultrasonication device (MEF391, Melfiz, Russia) for 10 min to ensure homogeneity of the probe, as was concluded from the stability of particle size distributions in a series of probes. After each cycle, fugate was separated and, after analysis, used for further treatment. The sediment was rinsed with acetone (99.5+%, Ecos-1, Russia), dried at 100 °C and weighed (Ohaus Ohaus P224/E, Ohaus, Parsippany, NJ, USA) in order to calculate and correct concentrations. Sufficiently centrifuged suspensions were transparent and yellow in colour. Residual concentration was estimated by carefully measuring the mass of the sediment. Hybrid suspensions were prepared by simple mixing of graphene aqueous suspensions and AgNP suspension in EG followed by ultrasonication for 15 min to ensure homogeneity and reduce agglomeration.

Particle-size distributions for un-centrifuged suspensions were measured via a laser diffraction (ISO 13320:2020) technique using Microtrac MRB SYNC apparatus (Microtrac, Osaka, Japan). For centrifuged suspensions, distributions were obtained via dynamic laser scattering (Nanosizer, Malvern Pananalytical, Malvern, UK). Quartz cuvettes were used for measurements (optical path length 10 mm).

Electrical conductivity measurements were performed with a SevenCompact conductometer equipped with InLab 710 glass/platinum electrodes (Mettler Toledo, Greifensee, Switzerland); 20 mL aliquots of suspensions were used. Sheet resistance was estimated via an IEC/TS 62607-2-1-2017-compatible 4-electrode method. We used copper electrodes and a b2901a precision source/measure unit (Keysight, Santa Rosa, CA, USA). Films were drop-casted (F1-ClipTip GLP, Thermo Scientific, Waltham, MA, USA) on glass substrates, and sintering was performed at 150 °C. Resistance was calculated from V-I curves (linear region slope at 0 V).

Optical spectra were recorded using a Cary 60 UV-vis spectrometer (Agilent, Santa Clara, CA, USA). All spectra were plotted for the 200–1100 nm range at 0.4 nm wavelength resolution. All as-synthetized suspensions were diluted 100 times in order to decrease absorption, while centrifuged suspensions were used as prepared. Quartz cuvettes were used for measurements (optical path length 10 mm).

TEM images were taken using a HT7800 (Hitachi, Tokyo, Japan) unit operating at a 100 kV accelerating voltage. SEM images were obtained using TM4000 unit (Hitachi, Japan) at 15 kV accelerating voltage.

3. Results and Discussion

3.1. Manufacturing of Graphene/AgNP Hybrid Suspensions

A step-by-step scheme for a hybrid manufacturing process is shown in Figure 1.

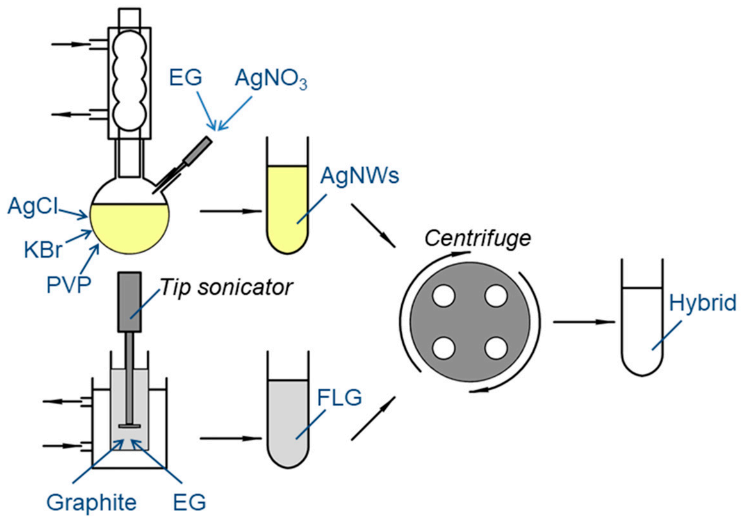

Figure 1. Process scheme for hybrid FLG/AgNPs suspensions manufacturing.

Polyol synthesis is widely used to manufacture suspensions of AgNPs of pre-defined morphologies [49–51], as suspensions can be readily formed into thin films suitable for various TCE applications [52–56]. In our previous study [48], we established that synthesis in EG at temperatures below 170 °C at a PVP/$AgNO_3$ weight ratio above 3:2 g/g leads to primarily silver nanowires (AgNWs) (Figure 2a,b); some smaller polyhedric and spherical AgNPs (Figure 2c; see also smaller particles in Figure 2b) are also present in the mixture. Such a complex suspension composition may seem detrimental, as usually efforts are made to obtain morphologically-homogeneous products [57–59], but numerous studies suggest that the percolation threshold is usually lower for composite systems of mixed particle morphology, as both experimental and theoretical studies suggest [60–62].

Direct liquid-phase exfoliation is a well-established protocol for manufacturing low-defect FLG at relatively low cost. Water-based suspensions of FLG can be effectively used as both fillers for polymer-based composites and thin film technology. As can be seen from Figure 2d, the technique described in detail in [47] provides very thin (2–3 layers) FLG with a lateral size of ca. 1 μm.

TEM images of particles in hybrid FLG/AgNP suspensions show very pronounced decoration of the FLG surface with smaller isometric silver particles. Although this decoration must be purely noncovalent in nature, it may well serve to increase composite connectivity while decreasing high FLG–FLG interparticle local contact resistances. The observed decoration effect was achieved by simple collective ultrasonication of the mixed suspension; therefore, no defects affecting π-electron system and charge carrier mobility should be introduced in the graphene plane. Analyzing electron microscopy data, one can also notice that in hybrid suspensions almost all of the FLG particles are decorated with AgNPs, which suggests a high homogeneity of the system.

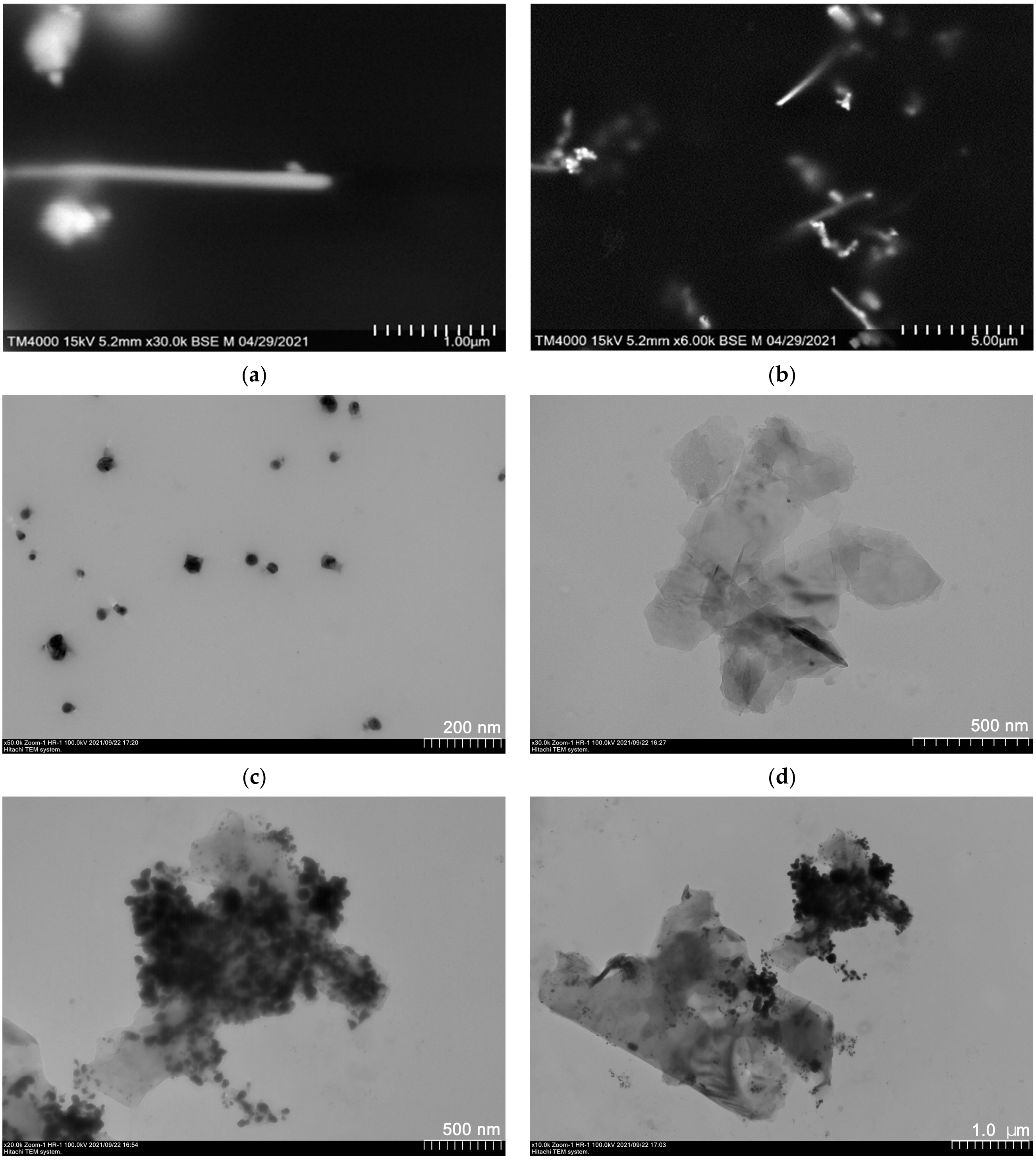

Figure 2. Electron microscopy data for nanoparticles used in the present work: (**a**,**b**) AgNWs, (**c**) polyhedral AgNPs, (**d**) FLG, (**e**,**f**) typical hybrid particles.

3.2. Influence of Centrifugation on Particle Size Distributions

As-obtained suspensions were opaque and non-transparent at any significant layer thickness (>1 mm). Transparent electrically conductive suspensions are a prerequisite for successful TCE manufacturing; therefore, it is of the utmost importance to reduce optical absorption while retaining most of the electrical conductivity (>100 μS/cm is usually a desired level for suspensions for printing technologies [63]). Particle-size distribution management is another major factor for electrically conductive suspensions intended for either inkjet printing or spray coating as agglomerates, and large particles may cause clogging of the nozzle; they may also have higher sintering temperatures, which may limit their applications for polymer substrates.

Centrifugation proved to be effective for separation of large particles and agglomerates [54,64,65] from FLG. In addition, it is also effective for increasing the average morphological homogeneity of particles in fugates [66], such as for separating FLG by the number of layers [67].

As can be readily seen from data in Figure 3a,b, centrifugation allows a two- to threefold reduction of mean particle size in AgNP suspensions. Symmetry of particle size distribution remain almost intact. As for FLG suspensions, the initial distribution is non-symmetrical, mean particle size being around 3–4 μm with a significant amount of small particles and a broad distribution of larger particles and agglomerates present (Figure 3c). After only mild centrifugation, particle size distribution becomes quite narrow and highly symmetrical with mean particle size reducing to ca. 0.5 μm (Figure 3d) (it generally varied in the range 0.5–1.5 μm from sample to sample). As for hybrid (mixed) FLG/AgNP suspensions, in an un-centrifuged state (see representative distribution in Figure 3e) they generally followed the distribution for FLG, as the particles are larger in size, and a relative decrease in size should be expected to be slower, since flakes have an increased coefficient of friction compared to rods and spheres [68].

After centrifugation, however, particle-size distribution does not resemble the sum of both components (see Figure 3f); while the primary maximum is that of FLG, no peak at ca. 0.3 μm attributed to AgNPs is observed. This fact is consistent with TEM observations (see Figure 2e,f), and one could state that AgNPs primarily decorate the surface of FLG with only excess smaller particles remaining freely suspended. The overall particle size distributions were clearly bimodal for all of the studied FLG/AgNPs ratios; therefore, in any case, although the peak attributed to FLG dominates the distribution, some AgNPs are not linked to the FLG surface (through non-covalent interactions, apparently [69]). This excess of AgNPs may lead to the increase in system connectivity in both suspensions and films.

It should also be noted that the initial FLG suspension concentration was 6.0 mg/mL, whereas for AgNPs it was 3.2 mg/mL. The average yield of the solid phase in centrifuged suspensions was 7.8 wt.% for FLG and ca. 15 wt.% for AgNPs, leaving centrifuged suspensions with bulk weight concentrations of 0.47 and 0.48 mg/mL, respectively (taking into account a not obvious assumption that centrifugation of particles in hybrid suspensions occurs independently). Nevertheless, as concentrations of the suspensions were relatively close, we took relative FLG content (wt.%), calculated as simply proportional to the initial FLG suspension weight in the mixture, to be the simple parameter to estimate the influence of the suspension composition on its properties.

Data for mean particle-size distributions as a function of suspension composition extracted from laser diffraction and dynamic laser scattering experiments are shown in Figure 4.

It can be readily seen that, except for the pure AgNP suspension, mean particle size matches that of FLG (2–4 μm) for all un-centrifuged suspensions. However, after centrifugation mean particle size does not only reduce, but also shows some dependence on suspension composition; at low FLG content it is close to that of pure AgNPs, which dominate in weight particle-size distribution. Then, around 50 wt.% of FLG content overall size matches that of FLG. At higher FLG concentrations (over 75 wt.%), mean particle size drops steadily. Although further research is needed, this effect may be partially explained by both a significant drop in liquid viscosity as the concentration of water in water/EG system increases, and increased average weight of AgNP-decorated FLG as compared to pure FLG (see data for 100 wt.% FLG content).

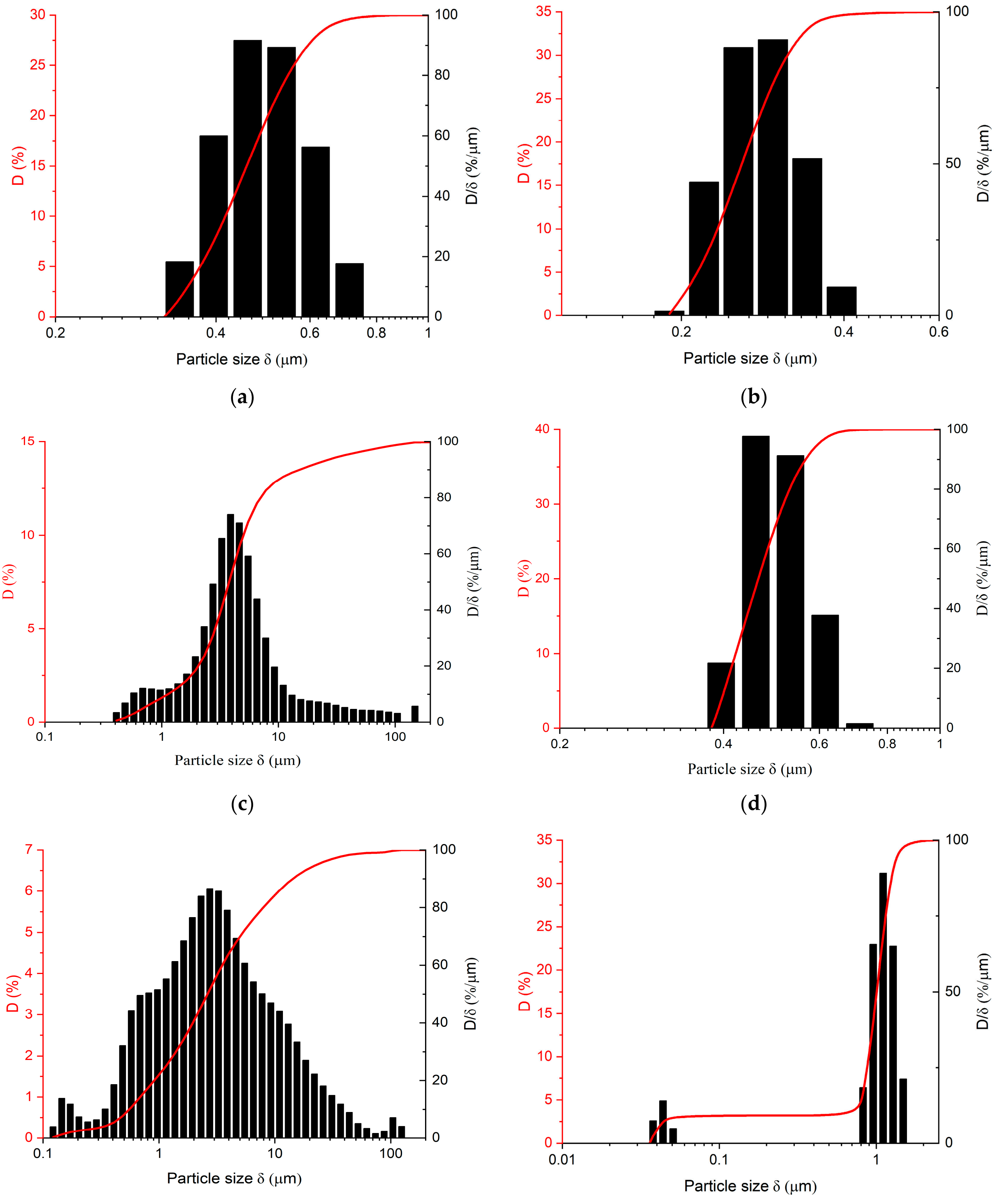

Figure 3. Particle-size distributions of the as-obtained (**a**,**c**,**f**) and centrifuged (30 min). (**b**,**d**,**e**) suspensions. (**a**,**b**) AgNPs, (**c**,**d**) FLG, (**e**,**f**) hybrid (75 wt.% FLG).

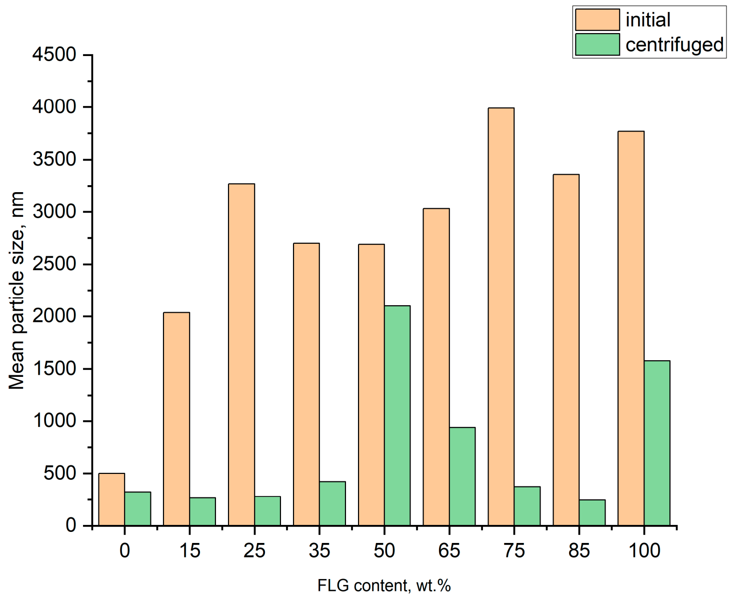

Figure 4. Mean particle size vs. FLG content for hybrid FLG/AgNP suspensions.

3.3. Non-Linear Concentration Effects of Optical Transparency and Electrical Conductivity

Initially we studied the influence of centrifugation and composition on suspension stability (Figure 5). Data suggest that centrifugation, although it leads to a significant decrease in suspension concentration (down to ca. 10 wt.% of the initial concentration), does not significantly affect a suspension's electrical conductivity. This was previously found for aqueous suspensions of pure FLG [70]. The fact that even after a serious decrease in concentration the electrical conductivity of suspensions remains almost intact may suggest two statements:

- Percolation threshold in the system (suspensions) is achieved even at concentrations as low as ca. 0.5 mg/mL (see Section 3.2); therefore, centrifugation does not significantly affect the level of electrical conductivity;
- Individual nanoparticles are primarily responsible for charge carrier properties in the suspensions; the influence of agglomerates and larger particles is not very pronounced.

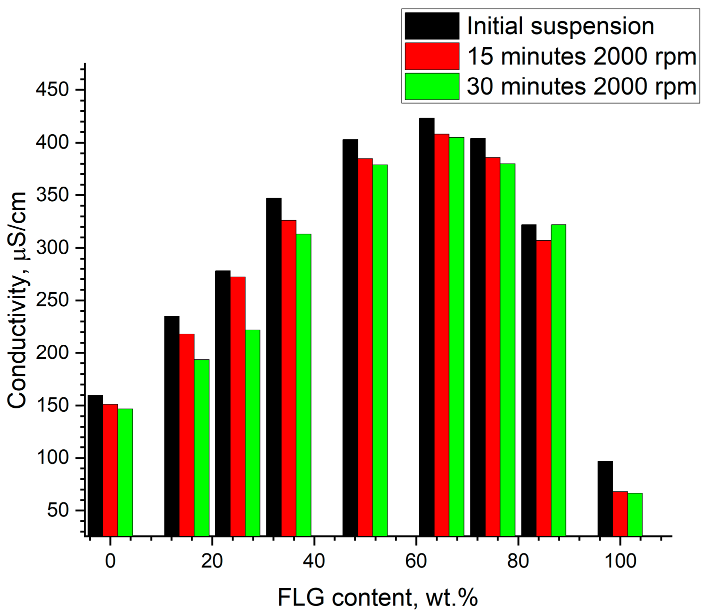

Figure 5. Specific electrical conductivity vs. FLG content for hybrid FLG/AgNPs suspensions.

Although a low percolation threshold [71,72] and network-like structuring of solid phase in suspensions [73] have been previously described for many, including graphene-based, systems, the latter statement requires more careful evaluation.

Data from Figure 5 suggest that, whereas initial AgNPs and FLG suspensions had electrical conductivity around 150 μS/cm and 100 μS/cm, respectively, the hybrid suspension containing 65 wt.% of FLG showed conductivity of almost 400 μS/cm independently of centrifugation. This non-linear concentration is obviously non-percolative in nature (overall concentration remains almost the same, and a sharp maximum with respect to both components concentration is observed); therefore, specific interactions between components in hybrid suspension should be responsible for the observed behavior.

A high level of local contact resistances is a well-known problem limiting potential electrical applications and achieving theoretical values of charge carrier properties for most semimetals, which include graphite-based materials and graphene [74]. In this particular case, the effect may be due to electrical bridging of FLG platelets through AgNPs, thus drastically decreasing contact resistance.

The non-linear concentration effect is also evident from optical transmission data (Figure 6). Optical spectra of centrifuged suspensions have two main features:

- Non-linear dependence of average transmission on suspension composition;
- Absence of the surface plasmon resonance (SPR) peak at 350–450 nm characteristic of AgNPs [75,76] (the peak is not very pronounced even at high AgNP loadings due to elevated overall optical absorption).

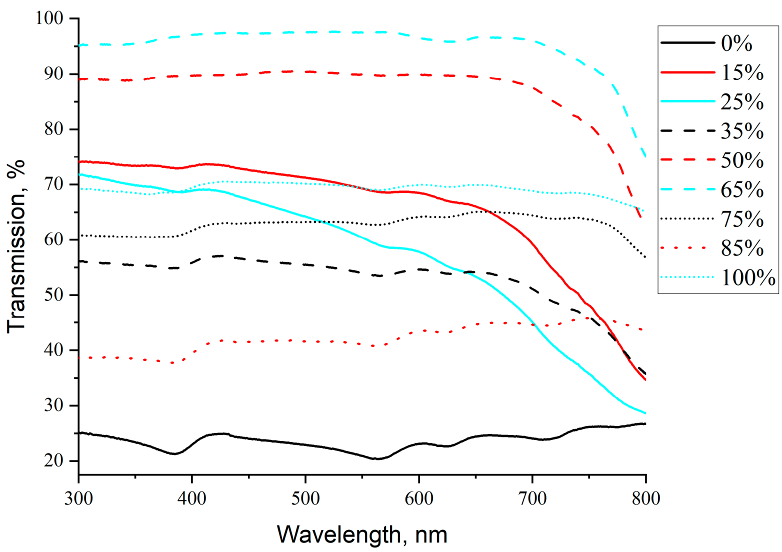

Figure 6. Optical transmission spectra for hybrid FLG/AgNPs suspensions at different component ratios (see legend).

Both of these feature specific mechanisms of carrier transport in the FLG/AgNP system that affect both direct current electrical conductivity and optics (i.e., interaction with a high-frequency electromagnetic field). Therefore, mixing and collectively ultrasonicating FLG and AgNP suspensions proves sufficient to provide interactions strong enough to significantly affect electrical and optical properties, as well as to reveal synergistic effects.

Figure 7 represents optical transmission data more clearly by showing suspensions' transmission at the red edge (950 nm), commonly used 650 nm, and blue edge (350 nm) of the visual region of the optical spectrum. It can be readily seen that throughout the whole visual region the maximal transmission is observed for the hybrid suspension containing 65 wt.% of FLG.

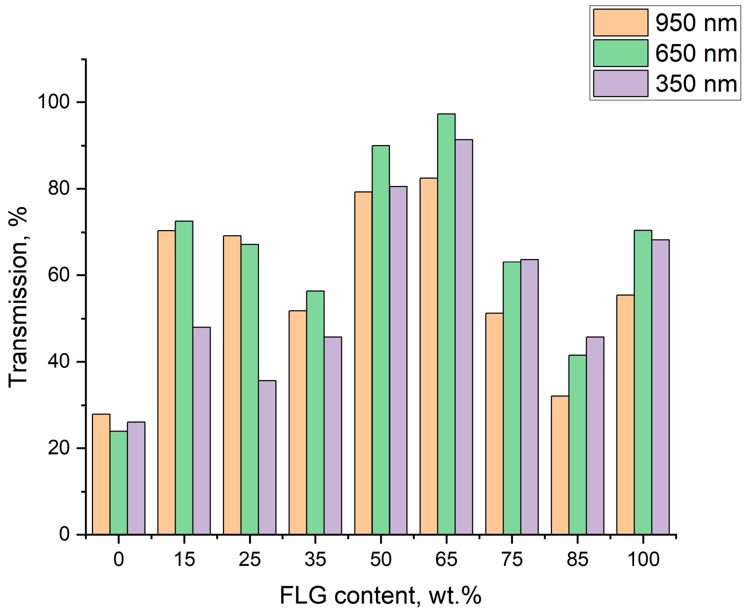

Figure 7. Optical transmission for FLG/AgNP-hybrid suspensions at different component ratios (wavelength—see legend).

The fact that the concentration correlation is evidently non-linear, as well as that the position of its maximum coincides for both electrical conductivity and light transmission, strongly suggests that indeed there is a link between these properties in the obtained suspensions, and that this should correlate with specific "network" and "bridging" structures, which obviously define charge carrier properties more significantly than only the concentration and morphology of the solid phase itself. Although this question deserves more careful evaluation, the effect is obvious, and both structural and bulk properties studies support this claim.

3.4. Electrical and Optical Properties of Graphene/AgNPs-Based Films

Hybrid suspensions manufactured in this work were used to obtain transparent films on glass substrates. Although comparison of the results of numerous studies suggest that the technology of film preparation greatly affects film properties, especially for carbon [77,78], metallic nanoparticles [77] and their hybrids [79,80], we used simple drop-casting in order to ascertain the effect of composition on structure-dependent properties formation.

Electrical properties were evaluated via analysis of the I-V curves measured using direct current and a 4-probe technique. Typical V-I curves are shown in Figure 8. It can be seen that all of the films behaved as linear resistors (as can be seen from the symmetric linear shape of the curve around zero point), which is consistent with TCE and contact track working conditions. It is noteworthy that concentration of the initial suspension seriously affects both the slope of the V-I curve around 0 V and the range of linearity, which generally tends to decrease at lower AgNP concentrations from ± 6 V at 15 wt.% FLG down to less than ± 1 V at 85 wt.%

Although the range of linearity is a very important property for microelectronics, sheet resistance is usually considered as a figure of merit for electrode-related applications [77–80]. In the current study, sheet resistance was estimated from resistance data defined as V-I curve slope around 0 V. It can be seen from Figure 9 that the plot is quite complex. Minimal resistance is seen for the pure AgNP film, which had poor optical properties. With an increase in FLG content (pure FLG film had the highest sheet resistance), one can observe a pronounced minimum once again around 65 wt.% of FLG content, which suggests that quantitative effects of AgNPs bridging FLG particles in the optimal concentration range hold true both in suspensions and in films.

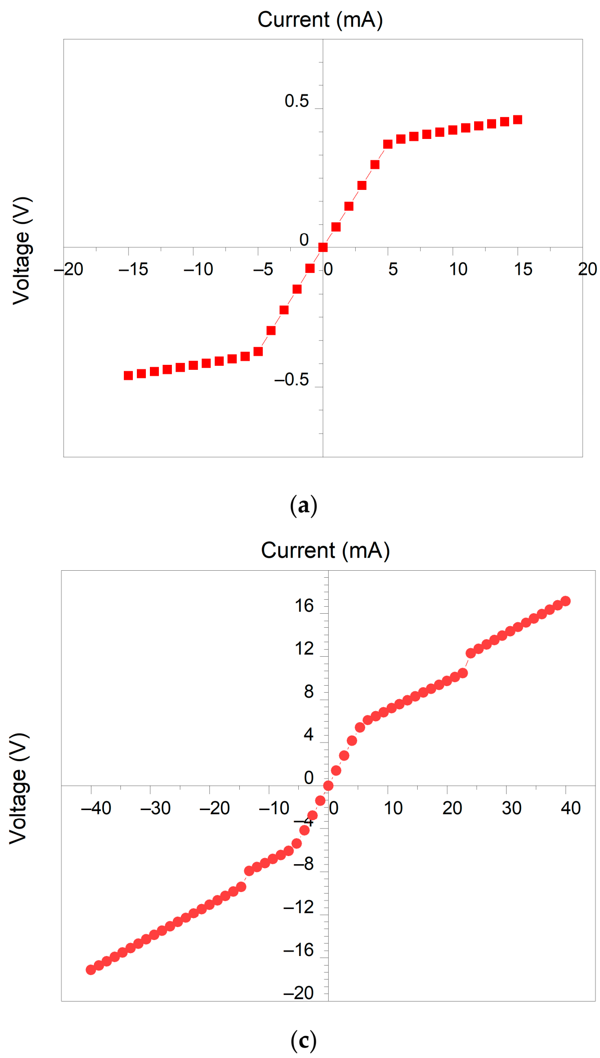

Figure 8. V-I curves of hybrid FLG/AgNPs films at 15 (**a**), 35 (**b**), 50 (**c**) and 85 wt.% (**d**) of FLG content.

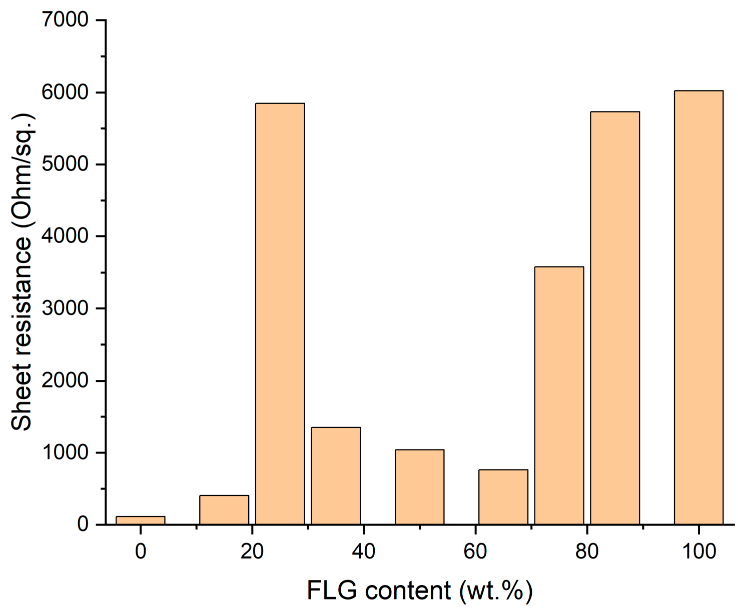

Figure 9. Sheet resistance of hybrid FLG/AgNPs films at different component ratios.

Figure 10 shows typical optical absorption spectra for different suspension compositions. Leaving aside the absolute values for transmission that may be attributed to technological aspects of film manufacturing, one can see that at least several spectra (e.g., for 65, 85 wt.% FLG) have pronounced SPR absorption; in this case, however, the overall absorption is significantly less than it is for pure AgNPs (0% FLG).

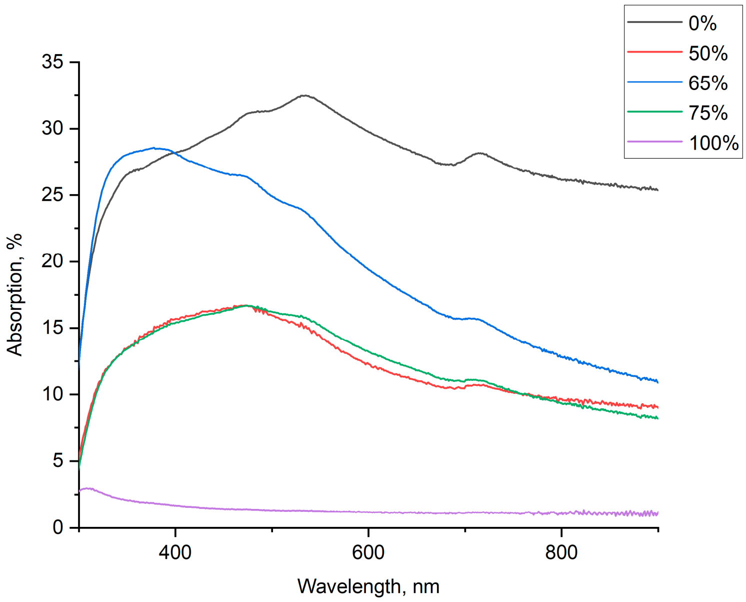

Figure 10. Optical absorption spectra for hybrid FLG/AgNP films at different component ratios.

Minimal absorption for hybrid suspensions (pure FLG was not considered) was observed for 50 and 75 wt.% of FLG. It can be concluded that, although it is close to the optimal value for suspensions (65 wt.%), interactions with light in hybrid thin films probably have certain differences as compared to suspensions, at least as long as interactions with an electromagnetic field are considered. Moreover, for films the SPR peak of AgNPs can be distinguished in most spectra.

Both these effects may be attributed to two main reasons. First, sintering leads to an increase in AgNP size and a subsequent change of optical properties. Second, interparticle interactions and network structure are most probably not equal in suspensions and films. Moreover, a simplistic film deposition technique can also affect the properties of the films; therefore, more advanced deposition techniques, such as the Langmuir-Blodgett [71], or spray-coating coupled with substrate pre-treatment, are suggested to test whether optimal FLG concentration in hybrid suspensions coincides with that in films as far as optical properties are examined.

Therefore, the question of the link between electrical and optical properties of hybrid FLG/AgNP system both in films and suspensions clearly needs to be more carefully examined; it is evident that there are specific interparticle interactions that provide non-linear effects with maximum properties around 65 wt.% FLG content. Therefore, the suspension composition and properties have a strong effect on the properties of thin films intended for use as TCE.

4. Conclusions

In the present study, the effect of FLG surface decoration with AgNPs after as much as collective ultrasonication was established. Particle-size distribution analysis suggests that mean particle size in centrifuged suspensions is mostly controlled by FLG, and only the smaller AgNPs remain freely suspended throughout the whole concentration range; therefore, simple collective ultrasonication provides both high homogeneity of the suspension and FLG decoration with AgNPs.

Hybrid FLG/AgNPs showed a pronounced synergistic effect of electrical conductivity and optical transparency at 65 wt.% of FLG, which cannot be explained by percolation and may be linked with bridging and structuring of the FLG–FLG interface through AgNPs. Optimal suspensions showed conductivity above 350 µS/cm at over 90% optical transparency in the visual region, which makes them a very promising ink material for TCE applications. Reported results significantly exceed most of the published data.

Hybrid films showed promising properties for TCE applications (sheet resistance below 1 KΩ/sq. at 90% transparency), although a straightforward drop-casting technique of film deposition was used; more elaborate techniques should be used in future. Minimal sheet resistance was observed at 65 wt.% of FLG; however, optical properties were higher for films containing 50 and 75 wt.% FLG. While the question of film property optimization requires further studies, it is evident that suspension properties define those of the films.

Author Contributions: Conceptualization, A.A.S., E.A.D. and V.S.; methodology, E.A.D. and M.V.; validation, M.V., T.K. and M.D.; formal analysis, E.A.D. and M.D.; investigation, E.A.D. and M.V.; data curation, E.A.D.; writing—original draft preparation, E.A.D., M.V. and T.K.; writing—review and editing, A.A.S., V.V.T. and E.A.D.; visualization, V.V.T., E.A.D., M.V. and T.K.; supervision, E.A.D. and V.S. All authors have read and agreed to the published version of the manuscript.

Funding: This work was supported by Ministry of science and higher education of Russia in the framework of state assignment number 075-00268-20-02 dated 12 March 2020, state program of basic research "For the long-term development and ensuring the competitiveness of society and the state" (47 GP) on the base of the universities, the plan for basic scientific research number 718/20 dated 6 March 2020, project number 0718-2020-0036.

Institutional Review Board Statement: Not applicable.

Informed Consent Statement: Not applicable.

Data Availability Statement: The data presented in this study are available on request from the corresponding author.

Acknowledgments: The authors would like to sincerely thank Igor Chistyakov (JSC "Scietegra") for access to high resolution SEM machine, as well as Aytan Muradova—for access to TEM machine.

Conflicts of Interest: The authors declare no conflict of interest.

References

1. Mu, B.; Xu, Y.; Xu, J.; Nikitina, M.A.; Zafari, U.; Xiao, X. Inkjet direct printing approach for flexible electronic. *Results Eng.* **2022**, *14*, 100466. [CrossRef]
2. Tran, T.S.; Dutta, N.K.; Choudhury, N.R. Graphene inks for printed flexible electronics: Graphene dispersions, ink formulations, printing techniques and applications. *Adv. Colloid Interf. Sci.* **2018**, *261*, 41–61. [CrossRef] [PubMed]
3. Lee, M.S.; Lee, K.; Kim, S.Y.; Lee, H.; Park, J.; Choi, K.H.; Kim, H.K.; Kim, D.G.; Lee, D.Y.; Nam, S.W.; et al. High-performance, transparent, and stretchable electrodes using graphene−metal nanowire hybrid structures. *Nano Lett.* **2013**, *13*, 2814–2821. [CrossRef]
4. Xue, Y.; Zhu, L.; Chen, H.; Qu, J.; Dai, L. Multiscale patterning of graphene oxide and reduced graphene oxide for flexible supercapacitors. *Carbon* **2015**, *92*, 305–310. [CrossRef]
5. Soni, M.; Kumar, P.; Pandey, J.; Sharma, S.K.; Soni, A. Scalable and site specific functionalization of reduced graphene oxide for circuit elements and flexible electronics. *Carbon* **2018**, *128*, 172–178. [CrossRef]
6. Wu, C.; Cheng, Q.; Wu, K. Electrochemical functionalization of N-methyl-2-pyrrolidone-exfoliated graphene nanosheets as highly sensitive analytical platform for phenols. *Analyt. Chem.* **2015**, *87*, 3294–3299. [CrossRef]
7. Wu, C.; Cheng, Q.; Wu, K.; Wu, G.; Li, Q. Graphene prepared by one-pot solvent exfoliation as a highly sensitive platform for electrochemical sensing. *Analyt. Chim. Acta* **2014**, *825*, 26–33. [CrossRef]
8. Li, J.; Ye, F.; Vaziri, S.; Muhammed, M.; Lemme, M.C.; Östling, M. A Simple Route towards High-Concentration Surfactant-Free Graphene Dispersions. *Carbon* **2012**, *50*, 3113–3116. [CrossRef]
9. Tyurnina, A.V.; Tzanakis, I.; Morton, J.; Mi, J.; Porfyrakis, K.; Maciejewska, B.M.; Grobert, N.; Eskin, D.G. Ultrasonic exfoliation of graphene in water: A key parameter study. *Carbon* **2020**, *168*, 737–747. [CrossRef]
10. Tyurnina, A.V.; Morton, J.A.; Subroto, T.; Khavari, M.; Maciejewska, B.; Mi, J.; Grobert, N.; Porfyrakis, K.; Tzanakis, I.; Eskin, D.G. Environment friendly dual-frequency ultrasonic exfoliation of few-layer graphene. *Carbon* **2021**, *185*, 536–545. [CrossRef]
11. Notley, S.M. Highly concentrated aqueous suspensions of graphene through ultrasonic exfoliation with continuous surfactant addition. *Langmuir* **2012**, *28*, 14110–14113. [CrossRef]

12. Narayan, R.; Kim, S.O. Surfactant mediated liquid phase exfoliation of graphene. *Nano Converg.* **2015**, *2*, 20. [CrossRef]
13. Morozov, Y.; Chistyakov, D.; Chernyshev, V.; Sergeev, G. Cryochemical synthesis of polymorphous nanostructures of a steroid neurohormone. *Molecules* **2017**, *22*, 1378. [CrossRef] [PubMed]
14. Skiba, M.; Pivovarov, A.; Vorobyova, V.; Derkach, T.; Kurmakova, I. Plasma-chemical formation of silver nanoparticles: The silver ions concentration effect on the particle size and their antimicrobial properties. *J. Chem. Technol. Metallurg.* **2019**, *54*, 311–318.
15. Cobley, C.M.; Skrabalak, S.E.; Campbell, D.J.; Xia, Y. Shape-controlled synthesis of silver nanoparticles for plasmonic and sensing applications. *Plasmonics* **2009**, *4*, 171–179. [CrossRef]
16. Khodashenas, B.; Ghorbani, H.R. Synthesis of silver nanoparticles with different shapes. *Arab. J. Chem.* **2019**, *12*, 1823–1838. [CrossRef]
17. Parente, M.; Van Helvert, M.; Hamans, R.F.; Verbroekken, R.; Sinha, R.; Bieberle-Hütter, A.; Baldi, A. Simple and fast high-yield synthesis of silver nanowires. *Nano Lett.* **2020**, *20*, 5759–5764. [CrossRef]
18. Li, J.; Ma, P.C.; Chow, W.S.; To, C.K.; Tang, B.Z.; Kim, J.K. Correlations between percolation threshold, dispersion state, and aspect ratio of carbon nanotubes. *Adv. Funct. Mater.* **2007**, *17*, 3207–3215. [CrossRef]
19. De, S.; King, P.J.; Lyons, P.E.; Khan, U.; Coleman, J.N. Size effects and the problem with percolation in nanostructured transparent conductors. *ACS Nano* **2010**, *4*, 7064–7072. [CrossRef]
20. Large, M.J.; Ogilvie, S.P.; Alomairy, S.; Vockerodt, T.; Myles, D.; Cann, M.; Chan, H.; Jurewicz, I.; King, A.A.K.; Dalton, A.B. Selective mechanical transfer deposition of Langmuir graphene films for high-performance silver nanowire hybrid electrodes. *Langmuir* **2017**, *33*, 12038–12045. [CrossRef]
21. Marcq, F.; Demont, P.; Monfraix, P.; Peigney, A.; Laurent, C.; Falat, T.; Courtade, F.; Jamin, T. Carbon nanotubes and silver flakes filled epoxy resin for new hybrid conductive adhesives. *Microelectron. Reliab.* **2011**, *57*, 1230–1234. [CrossRef]
22. Sagalianov, I.; Vovchenko, L.; Matzui, L.; Lazarenko, O. Synergistic enhancement of the percolation threshold in hybrid polymeric nanocomposites based on carbon nanotubes and graphite nanoplatelets. *Nanoscale Res. Lett.* **2017**, *12*, 140. [CrossRef] [PubMed]
23. Barani, Z.; Mohammadzadeh, A.; Geremew, A.; Huang, C.Y.; Coleman, D.; Mangolini, L.; Kargar, F.; Balandin, A.A. Thermal properties of the binary-filler hybrid composites with graphene and copper nanoparticles. *Adv. Funct. Mater.* **2019**, *30*, 1904008. [CrossRef]
24. Kim, K.W.; Han, W.; Kim, B.J. Effects of mixing ratio of hybrid carbonaceous fillers on thermal conductivity and mechanical properties of polypropylene matrix composites. *Polymers* **2022**, *14*, 1935. [CrossRef]
25. Birgin, H.B.; D'Alessandro, A.; Laflamme, S.; Ubertini, F. Hybrid carbon microfibers-graphite fillers for piezoresistive cementitious composites. *Sensors* **2021**, *21*, 518. [CrossRef]
26. Seiferling, F.; de las Heras, D.; Telo da Gama, M.M. Percolation in binary and ternary mixtures of patchy colloids. *J. Chem. Phys.* **2016**, *145*, 074903. [CrossRef]
27. Marsden, A.J.; Papageorgiou, D.G.; Vallés, C.; Liscio, A.; Palermo, V.; Bissett, M.A.; Young, R.J.; Kinloch, I.A. Electrical percolation in graphene–polymer composites. *2D Mater.* **2018**, *5*, 032003. [CrossRef]
28. Wang, Z.; Liu, H.; Chen, F.; Zhang, Q. A three-dimensional printed biomimetic hierarchical graphene architecture for high-efficiency solar steam-generation. *J. Mater. Chem. A* **2020**, *8*, 19387–19395. [CrossRef]
29. Liang, J.; Li, L.; Tong, K.; Ren, Z.; Hu, W.; Niu, X.; Chen, Y.; Pei, Q. Silver nanowire percolation network soldered with graphene oxide at room temperature and its application for fully stretchable polymer light-emitting diodes. *ACS Nano* **2014**, *8*, 1590–1600. [CrossRef]
30. Ferrari, A.G.M.; Rowley-Neale, S.J.; Banks, C.E. Screen-printed electrodes: Transitioning the laboratory in-to-the field. *Talanta Open* **2021**, *3*, 100032. [CrossRef]
31. Mallikarjuna, K.; Kim, H. Highly transparent conductive reduced graphene oxide/silver nanowires/silver grid electrodes for low-voltage electrochromic smart windows. *ACS Appl. Mater. Interf.* **2018**, *11*, 1969–1978. [CrossRef] [PubMed]
32. Miao, J.; Liu, H.; Li, W.; Zhang, X. Mussel-inspired polydopamine-functionalized graphene as a conductive adhesion promoter and protective layer for silver nanowire transparent electrodes. *Langmuir* **2016**, *32*, 5365–5372. [CrossRef] [PubMed]
33. Smith, S.L.; Nissamudeen, K.M.; Philip, D.; Gopchandran, K.G. Studies on surface plasmon resonance and photoluminescence of silver nanoparticles. *Spectr. Acta A Mol. Biomol. Spectr.* **2008**, *71*, 186–190. [CrossRef] [PubMed]
34. Gul, M.; Jelani, M.; Hassan, N.U.; Naeem, M.; Rakha, S.A.; Khurram, A.A.; Ali, N.; Munir, A. Modified electrical and microwave absorption properties of silver nanowires grown on graphene nanoplatelets. *Mater. Res. Express* **2019**, *6*, 1250f8. [CrossRef]
35. Zhang, N.; Wang, Z.; Song, R.; Wang, Q.; Chen, H.; Zhang, B.; Lv, H.; Wu, Z.; He, D. Flexible and transparent graphene/silver-nanowires composite film for high electromagnetic interference shielding effectiveness. *Sci. Bull.* **2019**, *64*, 540–546. [CrossRef]
36. Ray, A.; Narasimman, R. Transparent conducting electrodes for optoelectronic devices: State-of-the-art and perspectives. *Mater. Res. Found.* **2021**, *104*, 77–113.
37. Li, H.; Liu, Y.; Su, A.; Wang, J.; Duan, Y. Promising hybrid graphene-silver nanowire composite electrode for flexible organic light-emitting diodes. *Sci. Rep.* **2019**, *9*, 17998. [CrossRef]
38. Zhang, W.; Song, W.; Huang, J.; Huang, L.; Yan, T.; Ge, J.; Peng, R.; Ge, Z. Graphene: Silver nanowires composite transparent electrode based flexible organic solar cells with 13.4% efficiency. *J. Mater. Chem. A* **2019**, *7*, 22021–22028. [CrossRef]
39. Zhang, Y.; Bai, S.; Chen, T.; Yang, H.; Guo, X. Facile preparation of flexible and highly stable graphene oxide-silver nanowire hybrid transparent conductive electrode. *Mater. Res. Express* **2020**, *7*, 016413. [CrossRef]

40. Ye, N.; Yan, J.; Xie, S.; Kong, Y.; Liang, T.; Chen, H.; Xu, M. Silver nanowires-graphene hybrid transparent conductive electrodes for highly efficient inverted organic solar cells. *Nanotechnology* **2017**, *28*, 305402. [CrossRef]
41. Shin, D.H.; Seo, S.W.; Kim, J.M.; Lee, H.S.; Choi, S.H. Graphene transparent conductive electrodes doped with graphene quantum dots-mixed silver nanowires for highly-flexible organic solar cells. *J. Alloys Compd.* **2018**, *744*, 1–6. [CrossRef]
42. Duan, F.; Yang, W.J.; He, X.; Jiang, J.Y.; Zhu, W.Y.; Xia, D.X. Investigation on the silver nanowire/graphene transparent electrode in electrochromic device. *J. Nano Res.* **2018**, *55*, 82–90. [CrossRef]
43. Tugba Camic, B.; Vapaavuori, J.; Basarir, F. Transparent conductive electrode based on LBL deposition of graphene oxide and copper nanowires. *Mater. Lett.* **2022**, *311*, 131632. [CrossRef]
44. Huang, S.; Liu, Y.; Yang, F.; Wang, Y.; Yu, T.; Ma, D. Metal nanowires for transparent conductive electrodes in flexible chromatic devices: A review. *Envir. Chem. Lett.* **2022**, *20*, 3005–3037. [CrossRef]
45. Duan, F.; Li, W.; Wang, G.; Weng, C.; Jin, H.; Zhang, H.; Zhang, Z. Can insulating graphene oxide contribute the enhanced conductivity and durability of silver nanowire coating? *Nano Res.* **2019**, *12*, 1571–1577. [CrossRef]
46. Huang, H. Fabrication of three-dimensional sandwich-like silver nanowire network coated bilayer graphene nanostructures for flexible display. *Appl. Opt.* **2020**, *59*, 9878–9883. [CrossRef]
47. Samoilov, V.M.; Danilov, E.A.; Nikolaeva, A.V.; Yerpuleva, G.A.; Trofimova, N.N.; Abramchuk, S.S.; Ponkratov, K.V. Formation of graphene aqueous suspensions using fluorinated surfactant-assisted ultrasonication of pristine graphite. *Carbon* **2015**, *84*, 38–46. [CrossRef]
48. Danilov, E.A.; Dronova, M.A.; Veretennikov, M.R.; Samoilov, V.M.; Dulina, O.A.; Yashtulov, N.A. Influence of some synthesis medium parameters on particle size and properties of silver nanorods. *Vestn. Tehnol. Univ.* **2022**, *25*, 5–12. [CrossRef]
49. Ammar, S.; Fiévet, F. Polyol synthesis: A versatile wet-chemistry route for the design and production of functional inorganic nanoparticles. *Nanomaterials* **2020**, *10*, 1217. [CrossRef]
50. Cao, L.; Huang, Q.; Cui, J.; Lin, H.; Li, W.; Lin, Z.; Zhang, P. Rapid and facile synthesis of high-performance silver nanowires by a halide-mediated, modified polyol method for transparent conductive films. *Nanomaterials* **2020**, *10*, 1139. [CrossRef]
51. Fievet, F.; Ammar-Merah, S.; Brayner, R.; Chau, F.; Giraud, M.; Mammeri, F.; Peron, J.; Piquemal, J.Y.; Sicarda, L.; Viau, G. The polyol process: A unique method for easy access to metal nanoparticles with tailored sizes, shapes and compositions. *Chem. Soc. Rev.* **2018**, *47*, 5187–5233. [PubMed]
52. Kumar, A.; Shaikh, M.O.; Chuang, C.H. Silver nanowire synthesis and strategies for fabricating transparent conducting electrodes. *Nanomaterials* **2021**, *11*, 693. [CrossRef]
53. Li, B.; Ye, S.; Stewart, I.E.; Alvarez, S.; Wiley, B.J. Synthesis and Purification of Silver Nanowires to Make Conducting Films with a Transmittance of 99%. *Nano Lett.* **2015**, *15*, 6722–6726. [CrossRef]
54. Bao, J.; Wang, J.X.; Zeng, X.F.; Zhang, L.L.; Chen, J.F. Large-Scale Synthesis of Uniform Silver Nanowires by High-Gravity Technology for Flexible Transparent Conductive Electrodes. *Ind. Eng. Chem. Res.* **2019**, *58*, 20630–20638. [CrossRef]
55. Choi, Y.; Kim, C.S.; Jo, S. Spray deposition of Ag nanowire-graphene oxide hybrid electrodes for flexible polymer-dispersed liquid crystal display. *Materials* **2018**, *11*, 2231. [CrossRef] [PubMed]
56. Shi, Y.; He, L.; Deng, Q.; Liu, Q.; Li, L.; Wang, W.; Xin, Z.; Liu, R. Synthesis and applications of silver nanowires for transparent conductive films. *Micromachines* **2019**, *10*, 330. [CrossRef]
57. Liu, C.Y.; Zhang, Y.S.; Kao, C.K.; Liu, J.H. Fabrication of silver nanowires via a β-cyclodextrin-derived soft template. *Expr. Polym. Lett.* **2018**, *12*, 591–599. [CrossRef]
58. ZZhao, W.; Wang, S.S.; Cao, H.T.; Xie, L.H.; Hong, C.S.; Jin, L.Z.; Yu, M.N.; Zhang, H.; Zhang, Z.Y.; Huang, L.H.; et al. An eco-friendly water-assisted polyol method to enhance the aspect ratio of silver nanowires. *RSC Adv.* **2019**, *9*, 1933–1938. [CrossRef]
59. Chen, Z.; Balankura, T.; Fichthorn, K.A.; Riou, R.A. Revisiting the polyol synthesis of silver nanostructures: Role of chloride in nanocube formation. *ACS Nano* **2019**, *13*, 1849–1860. [CrossRef]
60. Gabbett, C.; Boland, C.S.; Harvey, A.; Vega-Mayoral, V.; Young, R.L.; Coleman, J.N. The effect of network formation on the mechanical properties of 1D:2D nano:nano composites. *Chem. Mater.* **2018**, *30*, 5245–5255. [CrossRef]
61. Barwich, S.; de Araújo, J.M.; Rafferty, A.; da Rocha, C.G.; Ferreira, M.S.; Coleman, J.N. On the relationship between morphology and conductivity in nanosheet networks. *Carbon* **2021**, *171*, 306–319. [CrossRef]
62. Cunningham, G.; Lotya, M.; McEvoy, N.; Duesberg, G.S.; van der Schoot, P.; Coleman, J.N. Percolation scaling in composites of exfoliated MoS_2 filled with nanotubes and graphene. *Nanoscale* **2012**, *4*, 6260–6264. [CrossRef] [PubMed]
63. Fernandes, I.J.; Aroche, A.F.; Schuck, A.; Lamberty, P.; Peter, C.R.; Hasenkamp, W.; Rocha, T.L. Silver nanoparticle conductive inks: Synthesis, characterization, and fabrication of inkjet-printed flexible electrodes. *Sci. Rep.* **2020**, *10*, 8878. [CrossRef] [PubMed]
64. Maragoó, O.M.; Bonaccorso, F.; Saija, R.; Privitera, G.; Gucciardi, P.G.; Iatií, M.A.; Calogero, G.; Jones, P.H.; Borghese, F.; Denti, P.; et al. Brownian motion of graphene. *ACS Nano* **2010**, *4*, 7515–7523. [CrossRef]
65. Torrisi, F.; Hasan, T.; Wu, W.; Sun, Z.; Lombardo, A.; Kulmala, T.S.; Hsieh, G.W.; Jung, S.; Bonaccorso, F.; Paul, C.J.; et al. Inkjet-printed graphene electronics. *ACS Nano* **2012**, *6*, 2992–3006. [CrossRef]
66. Danilov, E.A.; Samoilov, V.M.; Kalyakin, T.S.; Shakhnazarova, A.B.; Nakhodnova, A.V. Properties of suspensions of few-layer graphene particles obtained by means of the direct exfoliation of natural graphite in polyatomic alcohols. *Sorbtsionnye Khromatograficheskie Protsessy* **2022**, *22*, 453–465.
67. Gomez, C.V.; Tene, T.; Guevara, M.; Usca, G.T.; Colcha, D.; Brito, H.; Molina, R.; Bellucci, S.; Tavolaro, A. Preparation of few-layer graphene dispersions from hydrothermally expanded graphite. *Appl. Sci.* **2019**, *9*, 2539. [CrossRef]

68. Douglas, J.; Zhou, H.X.; Hubbard, J. Hydrodynamic friction and the capacitance of arbitrarily shaped objects. *Phys. Rew. E Stat. Phys. Plasm. Fluids Rel. Interd. Top.* **1994**, *49*, 5319–5331. [CrossRef]
69. Tang, X.Z.; Li, X.; Cao, Z.; Yang, J.; Wang, H.; Pu, X.; Yu, Z.Z. Synthesis of graphene decorated with silver nanoparticles by simultaneous reduction of graphene oxide and silver ions with glucose. *Carbon* **2013**, *59*, 93–99. [CrossRef]
70. Danilov, E.A.; Samoilov, V.M.; Dmitrieva, V.S.; Nikolaeva, A.V.; Ponomareva, D.V.; Timoshchuk, E.I. Manufacturing transparent conducting films based on directly exfoliated graphene particles via Langmuir-Blodgett technique. *Inorg. Mater. Appl. Res.* **2018**, *9*, 794–802. [CrossRef]
71. Lee, E.; Choi, K.B.; Lee, S.; Kim, J.; Jung, J.; Baik, S.; Lim, Y.; Kim, S.; Shim, W. A scalable and facile synthesis of alumina/exfoliated graphite composites by attrition milling. *RSC Adv.* **2015**, *5*, 93267–93273. [CrossRef]
72. Oskouyi, A.; Sundararaj, U.; Mertiny, P. Tunneling conductivity and piezoresistivity of composites containing randomly dispersed conductive nano-platelets. *Materials* **2014**, *7*, 2501–2521. [CrossRef] [PubMed]
73. Kazemi, F.; Mohammadpour, Z.; Naghib, S.M.; Zare, Y.; Rhee, K.E. Percolation onset and electrical conductivity for a multiphase system containing carbon nanotubes and nanoclay. *J. Mater. Res. Technol.* **2021**, *15*, 1777–1788. [CrossRef]
74. Srivastava, S.; Kinoa, H.; Joachima, C. Contact conductance of a graphene nanoribbon with its graphene nano-electrodes. *Nanoscale* **2016**, *8*, 9265–9271. [CrossRef]
75. Chen, D.; Qiao, X.; Qiu, X.; Che, J. Synthesis and electrical properties of uniform silver nanoparticles for electronic applications. *J. Mater. Sci.* **2009**, *44*, 1076–1081. [CrossRef]
76. Wang, G. Confronting theoretical results of localized and additional surface plasmon resonances in silver nanoparticles with electron energy-loss spectroscopy measurements. *Phys. Rev. B* **2021**, *103*, 195417. [CrossRef]
77. Kulkarni, G.U.; Kiruthika, S.; Gupta, R.; Rao, K.D.M. Towards low cost materials and methods for transparent electrodes. *Curr. Opin. Chem. Eng.* **2015**, *8*, 60–68. [CrossRef]
78. Xu, Y.; Liu, J. Graphene as transparent electrodes: Fabrication and new emerging applications. *Small* **2016**, *12*, 1400–1419. [CrossRef]
79. Luo, M.; Liu, Y.; Huang, W.; Qiao, W.; Zhou, Y.; Ye, Y.; Chen, L.S. Towards flexible transparent electrodes based on carbon and metallic materials. *Micromachines* **2017**, *8*, 12. [CrossRef]
80. Karim, N.; Afroj, S.; Tan, S.; Novoselov, K.S.; Yeates, S.G. All inkjet-printed graphene-silver composite inks for highly conductive wearable E-textiles applications. *Sci. Rep.* **2019**, *9*, 8035. [CrossRef]

Disclaimer/Publisher's Note: The statements, opinions and data contained in all publications are solely those of the individual author(s) and contributor(s) and not of MDPI and/or the editor(s). MDPI and/or the editor(s) disclaim responsibility for any injury to people or property resulting from any ideas, methods, instructions or products referred to in the content.